pharmaceutics

MDPI

Article

Evaluation of the Drug–Drug Interaction Potential of Cannabidiol Against UGT2B7-Mediated Morphine Metabolism Using Physiologically Based Pharmacokinetic Modeling

Shelby Coates [1], Keti Bardhi [1], Bhagwat Prasad [1] and Philip Lazarus [1,2,*]

[1] Department of Pharmaceutical Sciences, College of Pharmacy and Pharmaceutical Sciences, Washington State University, 412 E Spokane Falls Blvd., Spokane, WA 99202, USA
[2] Division of Quantitative Molecular Biosciences, Department of Pharmaceutical Sciences, School of Pharmacy and Pharmaceutical Sciences, SUNY University at Buffalo, 160 Hayes Rd., Buffalo, NY 14215, USA
* Correspondence: plazarus@buffalo.edu

Abstract: Background: Morphine is a commonly prescribed opioid analgesic used to treat chronic pain. Morphine undergoes glucuronidation by UDP-glucuronosyltransferase (UGT) 2B7 to form morphine-3-glucuronide and morphine-6-glucuronide. Morphine is the gold standard for chronic pain management and has a narrow therapeutic index. Reports have shown that chronic pain patients have increasingly used other supplements to treat their chronic pain, including cannabidiol (CBD). Up to 50% of chronic pain patients report that they co-use cannabis with their prescribed opioid for pain management, including morphine. Previous work has shown that cannabidiol is a potent inhibitor of UGT2B7, including morphine-mediated metabolism. Co-use of morphine and CBD may result in unwanted drug–drug interactions (DDIs). **Methods:** Using available physiochemical and clinical parameters, morphine and CBD physiologically based pharmacokinetic (PBPK) models were developed and validated in both healthy and cirrhotic populations. Models for the two populations were then combined to predict the severity and clinical relevance of the potential DDIs during coadministration of both morphine and CBD in both healthy and hepatic-impaired virtual populations. **Results:** The predictive DDI model suggests that a ~5% increase in morphine exposure is to be expected in healthy populations. A similar increase in exposure of morphine is predicted in severe hepatic-impaired populations with an increase of ~10. **Conclusions:** While these predicted increases in morphine exposure are below the Food and Drug Administration's cutoff (1.25-fold increase), morphine has a narrow therapeutic index and a 5–10% increase in exposure may be clinically relevant. Future clinical studies are needed to fully characterize the clinical relevance of morphine-related DDIs.

Keywords: physiologically based pharmacokinetic modeling (PBPK); UDP-glucuronosyltransferase (UGT); cannabidiol; cannabinoid; morphine; IVIVE; drug–drug interaction (DDI); cannabis; opioid

Citation: Coates, S.; Bardhi, K.; Prasad, B.; Lazarus, P. Evaluation of the Drug–Drug Interaction Potential of Cannabidiol Against UGT2B7-Mediated Morphine Metabolism Using Physiologically Based Pharmacokinetic Modeling. *Pharmaceutics* **2024**, *16*, 1599. https://doi.org/10.3390/pharmaceutics16121599

Academic Editors: Przemysław J. Danek and Anna Haduch

Received: 21 November 2024
Revised: 9 December 2024
Accepted: 10 December 2024
Published: 16 December 2024

1. Introduction

Morphine is an opioid analgesic that is commonly used to treat moderate to severe chronic pain [1,2]. Morphine is still considered to be the "gold standard" in pain management care and in other medical settings [3]. Metabolism of morphine occurs primarily in the liver, where morphine undergoes glucuronidation by UDP-glucuronosyltransferase (UGT) 2B7 to form morphine-3-glucuronide and morphine-6-glucuronide [4,5]. UGT2B7-meditead metabolism is the primary metabolic pathway of morphine [6]. Morphine-3-glucuronide is not pharmacologically active; however, it is associated with negative side effects of morphine [7,8]. In contrast, morphine-6-glucuronide is pharmacologically active and is thought to contribute to morphine's efficacy [9,10].

Cannabidiol (CBD), a major cannabinoid found in the cannabis plant, is available 'over-the-counter', and is legal within the United States. Its synthetic form, Epidiolex^{TM}, is used for the treatment of Dravet's syndrome, Lennox–Gastaut syndrome, and tuberous

sclerosis complex [11]. CBD is commonly used to self-treat several ailments including pain, anxiety, and depression [12,13]. The combination of opioids and cannabis is increasingly common [14–16], with up to 40% of chronic pain patients supplementing their opioid pain regimen with cannabis, including CBD [17]. Since morphine is a narrow therapeutic index drug, it is important to investigate the potential pharmacokinetic DDIs that may arise from concomitant use of morphine and CBD.

Previous in vitro studies have shown that major cannabinoids and their metabolites inhibit both CYP and UGT enzymes, including morphine UGT2B7-mediated glucuronidation [18–23]. In vitro to in vivo extrapolation (IVIVE) using static mechanistic modeling was performed to determine the potential for a drug–drug interaction (DDI) to occur in vivo with coadministration of morphine and individual cannabinoids [21]. While static mechanistic modeling of potential DDIs is useful, it only takes into consideration a single inhibitor concentration (C_{max}), and thus, only predicts the potential for a DDI based upon the worst-case scenario. Dynamic modeling, such as physiologically based pharmacokinetic (PBPK) modeling, is increasingly used to predict DDIs and has been utilized in drug approval applications waivers by the FDA [24,25]. Dynamic modeling is the preferred method to investigating potential DDIs as it allows for both the substrate and inhibitor concentration–time profiles to be considered when predicting a DDI. Furthermore, static modeling only allows for a single inhibitor to be modeled, as compared to PBPK where multiple inhibitors can be examined against one substrate simultaneously. This generates a more accurate prediction of an in vivo scenario of the potential DDI, especially for cases where a drug is taken with a drug or natural product that contains multiples of compounds like cannabis.

Previous research has shown that CBD can inhibit numerous drug-metabolizing enzymes in vitro including cytochrome P450 (CYP)s, UGTs, and carboxylesterases (CES), with static and dynamic modeling indicating the potential for a DDI in vivo [18–23], and these interactions may be associated with disease state. Taylor et al. [26] found that people with mild, moderate, and severe hepatic impairment had up to 4-fold higher exposure (AUC and C_{max}) to CBD compared to healthy individuals. Furthermore, Watkins et al. [27] found that CBD can be hepatoxic as seen by elevated levels of alanine aminotransferase after 750 mg B.I.D. of CBD. After administration of Epidiolex™, this elevation in alanine aminotransferase elevation is dose-dependent from 10 to 20 mg/kg/day [28]. Due to CBD's safety profile and inherent physiochemical properties (high Log P), it is increasingly important to examine the potential for CBD-mediated DDIs. Based upon previous research, the objective of the current study was to use dynamic physiologically based pharmacokinetic (PBPK) modeling to further evaluate potential DDIs between CBD and morphine by developing and validating both morphine and CBD PBPK models and assess the magnitude of potential DDIs between CBD and morphine in both healthy and cirrhotic populations.

2. Materials and Methods

2.1. PBPK Model Development and Validation

All PBPK models were developed using Simcyp software version 23.1 (Simcyp, Sheffield, UK). Input parameters including physiochemical properties, blood binding, and pharmacokinetic parameters used to simulate the pharmacokinetics of each drug are listed in Supplemental Table S1 (morphine) and Supplemental Table S2 (CBD). Morphine's clearance profile was based on the model of Emoto et al. [29] and the advanced dissolution, absorption, and metabolism (ADAM) model for morphine based upon the model from Uchaipichat et al. (2022) [30]. The morphine model was developed and validated using the healthy adult population within Simcyp. A full PBPK model based upon Rodgers and Rowland's method [31,32] was used in simulations to predict morphine distribution. A permeability-limited liver model was used to describe morphine distribution within the liver [29,33,34]. This model included OCT1 transport in the liver and UGT2B7-mediated metabolism to M3G and M6G using optimized enzyme and transporter kinetics [29,35,36]. To model controlled-release (CR) formulations of morphine, the release profile was taken

from previous studies [37] and incorporated into the ADAM model. The model was also validated in a hepatically impaired population for both IV and oral formulations using the existing Simcyp model (Child–Pugh C) for severe hepatic impairment (HI). Brain tissue concentration was predicted after validation using cerebrospinal fluid (CSF) concentrations to model morphine exposure within the brain. P-glycoprotein CL_{int} was taken from Verscheijden et al. [38] and incorporated into a permeability-limited brain model. The passive permeability-surface area product (PSB) on the blood–brain barrier (BBB) and the passive permeability-surface area product on the blood–CSF barrier (PSC) were optimized to recapitulate the observed CSF morphine concentrations, where the PSC is expected to be half of the PSB (half the surface area) [39]. Morphine CSF concentration was used as a surrogate for morphine brain tissue concentration during model development due to lack of available clinical data of morphine concentration in the brain. The PBPK model development for CBD was based upon Bansal et al. [40] and can be found in the Supplementary Methods. Simulations were conducted using the Simcyp healthy volunteers' population, with a minimum of 400 subjects per trial; number of subjects, age, sex, route of administration, dose, and fed vs. fasted state were identical to those in the corresponding clinical study. Model predictive performance was evaluated by comparing the simulated area under the concentration–time curve (AUC) and maximum plasma concentration (C_{max}) to the observed in vivo data that were used as validation sets (not training sets). The model was validated if the predicted AUC and C_{max} values were within 0.5- to 2-fold the range of observed in vivo data. The model was further analyzed visually by comparing if the observed data points fell within the 95% confidence intervals (CIs) of the simulated concentration–time curve (WebPlotDigitizer v4.7; https://automeris.io/WebPlotDigitizer; URL accessed on 1 September 2023). Model validation was also statistically analyzed by determining the mean relative deviation (MRD) and geometric mean fold error (GMFE) of both the AUC and C_{max} predicted-to-observed ratios (Supplementary Methods).

2.2. DDI Prediction and Model Validation

Sensitivity analysis was performed to evaluate predictive model performance by decreasing the K_i values of CBD against morphine glucuronidation by 1- to 10-fold. It is expected that with decreasing K_i values the AUCR would increase.

DDI trials were simulated with 400 subjects (20 subjects × 20 trials) in healthy adults with an equal proportion of males and females, and an age range of 20–40 years. CBD oral doses (1500 mg twice daily) were administered for 7 days, while morphine was set as single IV and oral doses, which were co-administered with CBD on day 6. The IV, oral solution, immediate-release (IR) tablets, and controlled-release (CR) morphine doses were set at 3.76 mg, 11.7 mg, 15.2 mg, and 22.6 mg, respectively. The magnitude of the DDI is presented as the morphine AUC ratio when co-administered with CBD. DDI trials were also simulated with severe hepatic impairment with 400 subjects (20 subjects × 20 trials) with an equal proportion of females and an age range of 20–40 years.

3. Results

3.1. Morphine PBPK Model Validation After IV and Oral Administration

The PBPK model—predicted morphine plasma concentration—time profiles following IV, IR, and CR administration were comparable to the observed in vivo data used as training and validation datasets (Figure 1; Supplemental Figures S1 and S2). The mean GMFE and MRD predicted-to-observed AUC and C_{max} ratios were below the 2-fold cut off for all formulations (Supplemental Table S3). The mean GMFE and MRD predicted-to-observed AUC ratios for IV were 1.71 and 1.65, respectively (Supplemental Table S3). The mean GMFE and MRD predicted-to-observed AUC ratios were 2.00 and 1.96, and 1.96 and 1.95 for predicted-to-observed C_{max} ratios, for IR formulations, and were 2.00 and 1.70, and 1.95 and 1.42, for predicted-to-observed AUC and C_{max} ratios, respectively, for CR formulations (Supplemental Table S3). These results indicate successful development of a PBPK model for morphine after IV and oral administration that can simulate clinically observed pharma-

cokinetics of morphine. PBPK models accurately predicted morphine CSF concentrations after IV administration (Supplemental Figure S3) and GMFE/C_{max} and MRD/C_{max} ratios were below the 2-fold cut off (1.24 and 1.02, respectively; Supplemental Table S3). The predicted morphine brain concentration–time profile following IV administration is also shown and is slightly higher (21.32 ng/mL) than the predicted and observed morphine CSF concentrations (Supplemental Figure S3), suggesting that the CSF concentration may be a good surrogate for brain tissue concentrations.

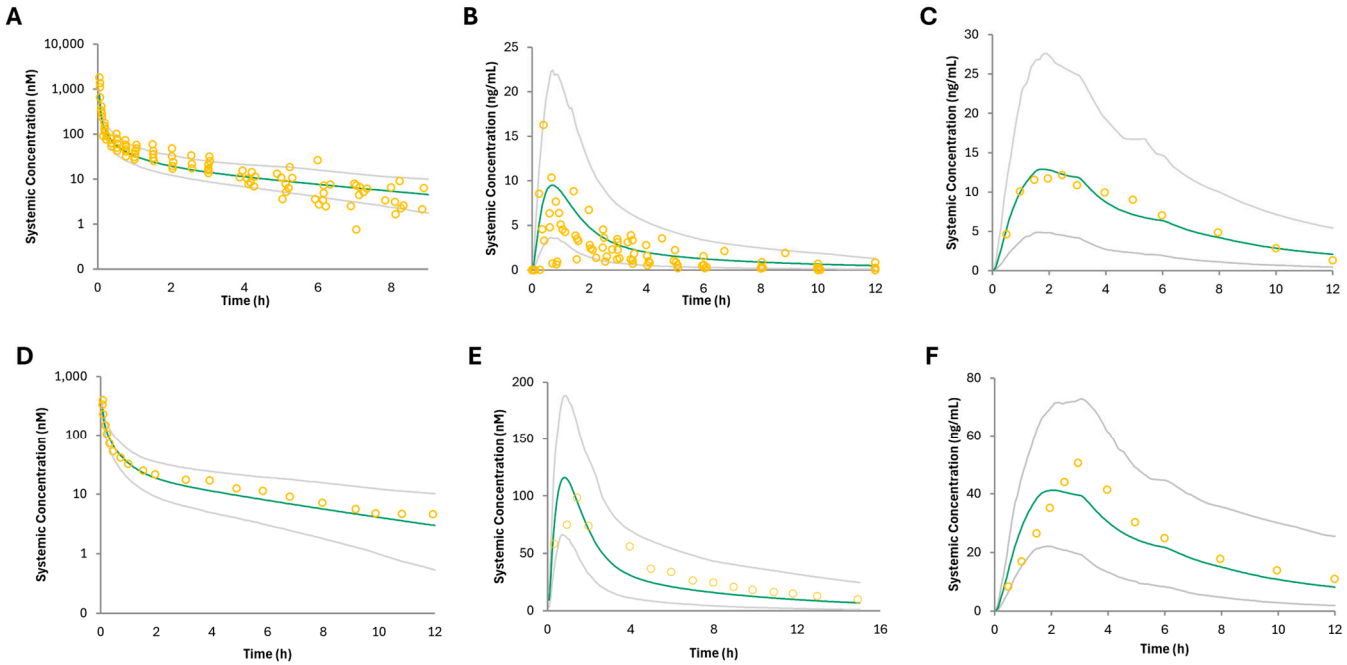

Figure 1. PBPK model of predicted and observed morphine plasma pharmacokinetic profiles after (**A**) IV (Lotsch et al., 2002) [41], (**B**) IR oral (Hoskin et al., 1989) [42], and (**C**) CR (Kotb et al., 2005) [43] oral administration in healthy adults and (**D**) IV (Hasselstrom et al., 1990) [44], (**E**) IR oral (Hasselstrom et al., 1990) [44], and (**F**) CR oral (Kotb et al., 2005) [43] administration in adults with cirrhosis. Data points are the observed values, and the green line represents the model's predicted morphine plasma concentration–time profile. Gray lines indicate the 5th–95th percentile of the virtual population.

3.2. CBD PBPK Model Validation After IV and Oral Administration

The PBPK model—predicted CBD plasma concentration—time profiles following IV and oral administration in both the fasted and fed states were comparable to the observed in vivo data used as a training dataset (Figure 2, Supplemental Figures S4 and S5). The GMFE and MRD predicted-to-observed AUC and C_{max} ratios were below 2, indicating an acceptable model (see Supplemental Table S4). The mean GMFE and MRD predicted-to-observed AUC ratios were 1.91 and 1.2, respectively, for IV (Supplemental Table S3). The mean GMFE and MRD predicted-to-observed AUC and C_{max} ratios were 1.87 and 1.49, and 1.59 and 1.35, respectively, for the fasted state, and 1.33 and 1.06, and 1.80 and 1.24, respectively, for the fed state, respectively (Supplemental Table S4). These results indicate successful development of a PBPK model for CBD after IV and oral administration that can simulate clinically observed pharmacokinetics of CBD. The CBD predicted plasma concentration–time profile following multiple doses of oral administration in the fasted state was comparable to the observed in vivo data (Figure 3). The GMFE and MRD predicted-to-observed AUC and C_{max} ratios were below the 2-fold cut off (Supplemental Table S4). The GMFE and MRD predicted-to-observed AUC and C_{max} ratios were 1.67 and 1.22, and 2.00 and 1.40, respectively, as compared to the observed AUC and C_{max} measured on days 1 and 7 after multiple dose administration of CBD to healthy subjects (Supplemental Table S4).

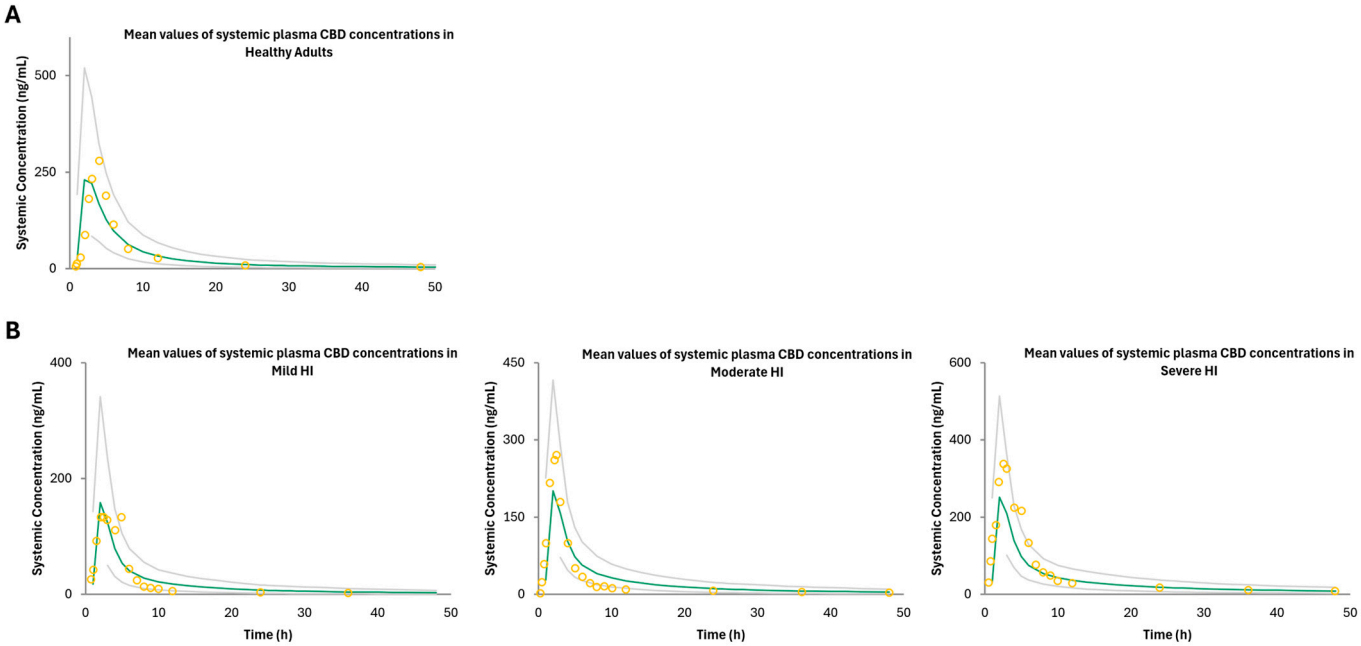

Figure 2. PBPK model of predicted and observed CBD plasma pharmacokinetic profiles after (**A**) oral administration in healthy adults (Taylor et al., 2018) [45] and (**B**) oral administration in adults with cirrhosis (Taylor et al., 2019) [26]. Data points are the observed values, and the green line represents the model-predicted morphine plasma concentration–time profiles. Gray lines indicate the 5th–95th percentile of the virtual population.

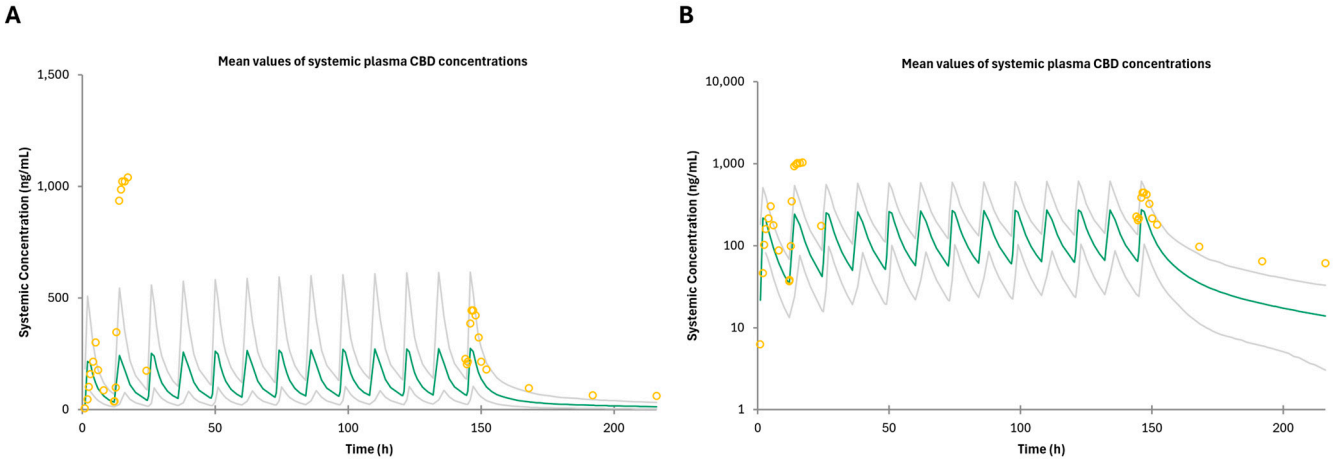

Figure 3. PBPK model of predicted and observed CBD plasma pharmacokinetic profiles after oral administration of 1500 mg twice daily for 7 days in healthy adults plotted on a (**A**) non-log, and (**B**) log scale. Data points are the observed values, and green the line represents the model-predicted CBD plasma concentration–time profile. Gray lines indicate the 5th–95th percentile of the virtual population.

3.3. PBPK Model Validation in Hepatic-Impaired Adult Populations

The PBPK model—predicted morphine plasma concentration—time profiles following IV and oral administration in cirrhotic populations (Child–Pugh C) were comparable to the observed in vivo data used for this analysis (Figure 1). The CR severe hepatic impairment model GMFE and MRD were greater than 2, indicating underprediction of both the AUC and C_{max}; the model is still considered acceptable based upon the other acceptance criteria (Supplemental Table S3). The mean GMFE and MRD predicted-to-observed AUC ratios for IV were 1.68 and 1.12, the mean GMFE and MRD predicted-to-observed AUC and C_{max} ratios for IR formulations were 2.30 and 1.35 (AUC) and 1.60 and 1.1 (C_{max}), and the

mean GMFE and MRD predicted-to-observed AUC and C_{max} ratios for CR formulations were 3.16 and 1.76 (AUC) and 2.21 and 1.32 (C_{max}) (Supplemental Table S3). The PBPK model—predicted CBD plasma concentration—time profiles following oral administration in mild, moderate, and severe hepatic impairment were comparable (> 0.5-fold of the observed AUC and C_{max}) to the observed in vivo data used (Figure 3; Supplemental Table S4). The GMFE and MRD predicted-to-observed AUC and C_{max} ratios for mild HI were 1.79 and 1.16 (AUC), 2.17 and 1.30 (C_{max}); the GMFE and MRD predicted-to-observed AUC and C_{max} ratios for moderate HI were 1.30 and 1.03 (AUC) and 2.86 and 1.61 (C_{max}); and the GMFE and MRD predicted-to-observed AUC and C_{max} ratios for severe HI were 1.93 and 1.20 (AUC) and 2.26 and 1.33 (C_{max}), with a combined GMFE and MRD of 1.70 and 1.27 for AUC, and 2.43 and 1.85 for C_{max}, respectively (Supplemental Table S4). Although the C_{max} GMFE for mild, moderate, and severe HI is greater than 2, indicating under prediction of the observed C_{max} compared to the simulation, the model is still considered acceptable based upon the other acceptance criteria and similar findings in Bansal et al.'s HI models [40].

3.4. PBPK Model for DDI Simulation with Coadministration of Morphine and CBD

The validated PBPK models for morphine and CBD were combined to predict the magnitude of the potential DDI arising from inhibition of morphine glucuronidation by CBD in a virtual healthy population and severe HI population. Due to the lack of clinical data investigating this potential DDI for model validation, sensitivity analysis was employed to evaluate model robustness; decreasing the K_i value (1–10-fold) may increase the ratio of simulate morphine AUC. As shown in Supplemental Figure S6, reduced K_i values for CBD against morphine glucuronidation in healthy subjects resulted in an expected increase in the simulated morphine AUC in both IV and oral administration models.

Based upon virtual trials with healthy subjects, coadministration of CBD (1500 mg twice daily for 7 days) and 11.7 mg of morphine (oral solution) or 15.2 mg of IR morphine leads to a mild increase in morphine exposure and C_{max} (6%; Table 1; Supplemental Figure S7). Based upon virtual trials with subjects with severe hepatic impairment, coadministration of CBD (1500 mg twice daily for 7 days) and either 11.7 mg of morphine (oral solution) or 15.2 mg of IR morphine also leads to a mild increase in morphine exposure and C_{max} (7% and 6%, respectively; Table 1; Supplemental Figure S7). In virtual trials with healthy subjects, coadministration of CBD (1500 mg twice daily for 7 days) with 22.6 mg of CR oral morphine led to an AUCR and C_{max} ratio of 1.04 and 1.05, respectively, while the trials in an adult population with severe hepatic impairment with coadministration of CBD saw an AUCR and C_{max} ratio of 1.06 (Table S1).

Table 1. PBPK-model-predicted and observed (mean and 95% CI) morphine exposure in healthy and cirrhotic populations with and without CBD administration.

		Sim-Healthy			
	Dose (mg)	**AUC (ng·h/mL)**	**95% CI**	**C_{max} (ng/mL)**	**95% CI**
Morphine Solution					
Morphine	11.7	36.8	34.9–38.9	12.7	12.2–13.3
Morphine + CBD		39.0	37.0–41.2	13.5	13.0–14.1
Obs/Pred Ratio		1.06		1.06	
Morphine IR					
Morphine	15.2	48.4	45.8–51.0	16.8	16.0–17.5
Morphine + CBD		51.2	48.5–5430	17.8	17.0–18.6
Obs/Pred Ratio		1.06		1.06	
Morphine CR					
Morphine	22.6	70.0	66.3–73.9	11.4	10.9–11.9
Morphine + CBD		72.6	68.8–76.6	11.9	11.4–12.5
Obs/Pred Ratio		1.04		1.05	

Table 1. *Cont.*

	Sim-Cirrhosis				
	Dose (mg)	**AUC (ng·h/mL)**	**95% CI**	**C_{max} (ng/mL)**	**95% CI**
Morphine Solution					
Morphine	11.7	119.1	113.9–124.6	39.4	38.2–40.5
Morphine + CBD		127.9	122.2–133.9	41.7	40.5–43.0
Obs/Pred Ratio		1.07		1.06	
Morphine IR					
Morphine	15.2	155.7	148.9–162.8	51.5	50.0–53.0
Morphine + CBD		167.0	159.6–174.9	54.5	52.9–56.1
Obs/Pred Ratio		1.07		1.06	
Morphine CR					
Morphine	22.6	223.7	213.9–234.0	37.1	36.0–38.3
Morphine + CBD		236.3	225.8–247.4	39.2	37.9–40.5
Obs/Pred Ratio		1.06		1.06	

Abbreviations: IR—immediate release; CR—controlled release; AUC—area under the plasma concentration–time curve; C_{max}—maximum plasma concentration; Obs/Pred Ratio—Observed/Predicted ratio.

Predicted morphine brain tissue concentrations after concomitant administration of CBD and morphine in healthy adults and adults with cirrhosis increased by 6% and 9% after administration of each formulation of morphine (Figure 4). Furthermore, the active metabolite, morphine-6-glucuronide, concentrations decreased after administration of CBD. Based upon (intrinsic organ clearance) CL_{int} in the liver, kidney, and the gut—the DDI has the largest impact in the small intestine (Figure 5) in healthy populations with a decrease in CL_{int} by 21.8%, whereas the largest decrease in CL_{int} occurred in the kidneys (21.4%) in HI populations.

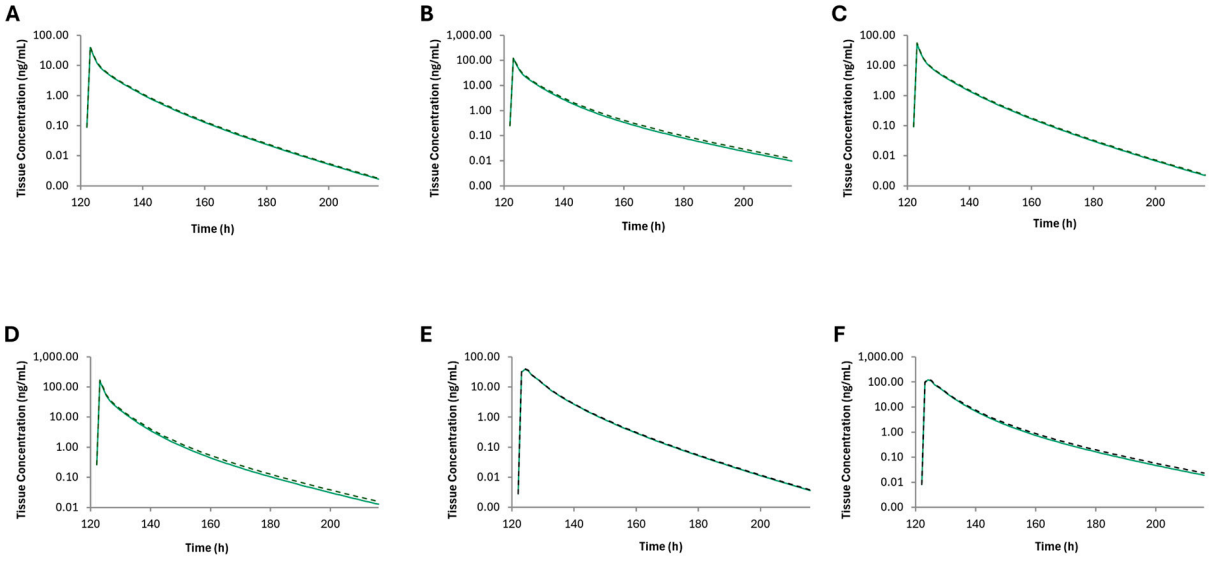

Figure 4. Brain tissue concentrations of morphine after oral administration of (**A**) oral solution (11.7 mg) in healthy adults, (**B**) oral solution (11.7 mg) in adults with severe hepatic impairment, (**C**) immediate-release tablet (15.2 mg) in healthy adults, (**D**) immediate-release tablet (15.2 mg) in adults with severe hepatic impairment, (**E**) controlled-release tablet (22.6 mg) in healthy adults, and (**F**) controlled-release tablet (22.6 mg) in adults with severe hepatic impairment. Shown are the mean brain morphine concentrations with (black dashed line or without (green line) cannabidiol over time.

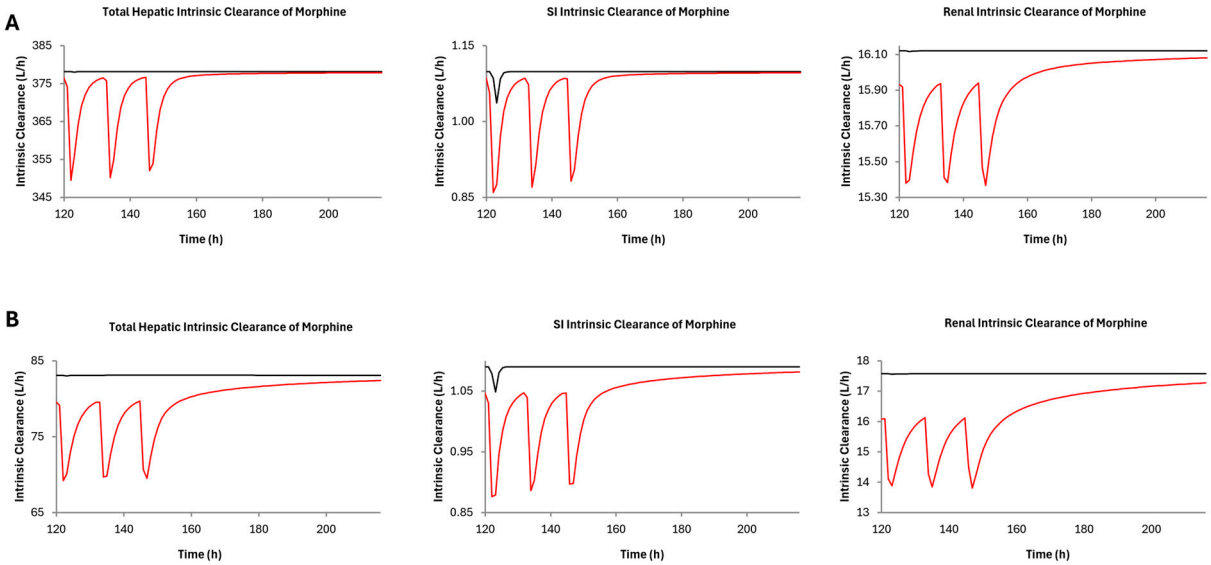

Figure 5. Morphine intrinsic clearance (CL_{int}) after CBD administration (1500 mg twice daily for 7 days) with 15.2 mg of immediate-release morphine in (**A**) healthy and (**B**) hepatically impaired adults. The red and black lines represent morphine CL_{int} with and without the presence of CBD, respectively. There was a 7.6, 21.8, and 4.8% decrease in hepatic, small intestine, and renal CL_{int}, respectively, in healthy adults, and a 17.2, 19.6, and 21.4% decrease in hepatic, small intestine, and renal CL_{int}, respectively, in adults with cirrhosis.

4. Discussion

Our previous in vitro studies have found that major cannabinoids, including CBD and their metabolites, inhibit UGT2B7-mediated metabolism of multiple substrates, including zidovudine, oxazepam, and morphine [19–21]. Utilizing static mechanistic modeling as recommended by the FDA [21,46], it was found that major cannabinoids, specifically CBD, could potentially cause DDI when co-administered with morphine (AUCR $\geq$ 1.25). However, results from the present study using PBPK models indicate less dramatic inhibition of morphine UGT2B7-mediated metabolism by CBD. While only a 5–10% increase in morphine exposure was predicted with PBPK models in both healthy and cirrhotic populations, this increase in morphine exposure may still be clinically relevant. Like all opioids, morphine has a narrow therapeutic index [47], and a major adverse side effect of morphine use is respiratory depression. Thus, while a 5–10% increase may not be classified as a clinically relevant DDI pharmacokinetically as defined by the FDA [46], such an increase could lead to increases in morphine concentrations in the brain that may lead to changes in pharmacodynamic effects. This may be clinically relevant and could lead to increased respiratory depression or overdose, varying between individuals. Therefore, morphine dose adjustments or adjustments in the frequency of morphine administration may still be necessary during coadministration with CBD to ensure patient safety. Furthermore, individuals who are taking morphine to manage their chronic pain are likely part of a patient population that takes multiple medications simultaneously, further increasing the risk for DDI and the need for dose adjustments as the effects of other concomitant drugs on this interaction should be considered. Therefore, it is prudent for clinicians to monitor patients who concomitantly use CBD and morphine to ensure that morphine plasma concentrations are within the therapeutic window.

Results from the present study are similar to Uchaipichat et al., where PBPK modeling was used to determine the potential for a DDI between morphine and diclofenac and S-naproxen [30]. Minimal increases in morphine exposure were observed with coadministration of S-naproxen (1–13%) [30,46]. However, they noted that a mild increase in morphine exposure may still be clinically relevant due to the narrow therapeutic window of morphine [30].

The CBD models used to simulate morphine exposure in mild, moderate, and severe HI varied from the model described in Bansal et al. [40]. The previously reported CBD model incorporated proteomic data changes in the total abundance of both UGT1A9 and UGT2B7 to model CBD exposure in the three HI populations (Child–Pugh A-C) within Simcyp as Simcyp V20 had yet to incorporate UGT total abundance into models [40]. However, the current version of Simcyp V23 does incorporate UGT abundance changes in Child–Pugh A-C models. In the present study, the CBD HI models described previously [40] were confirmed by comparing the default Child–Pugh A and B Simcyp model which incorporates UGT enzyme abundance vs. the values used from El-Khateeb et al., improving recapitulation of observed data (see Figure 3) [48]. However, the abundance changes previously reported were used for the Child–Pugh C model as the predicted exposure of CBD based on those abundance values best fit the observed data (Figure 3). The default Child–Pugh C model incorporating UGT2B7 abundance values best described the morphine cirrhotic population data and was used for DDI modeling.

Hepatic impairment appeared to have little effect on the potential DDI between morphine and CBD. Uchaipichat et al. also found similar results where the increase in morphine exposure after administration with the perpetrator drug was less in cirrhotic populations compared to healthy volunteers [30]. This is contradictory to previous pharmacokinetic studies where morphine exposure increased, and the hepatic extraction ratio decreased in cirrhotic patients [44,49–51]. However, one study found no difference in morphine exposure and hepatic extraction in cirrhosis patients compared to healthy controls [52]. The difference between these studies could be due to the severity of liver cirrhosis in the patients in each of these studies.

Hasselström et al. found that dosage reduction is needed in cirrhotic patients who are prescribed morphine to avoid toxicity and adverse side effects [44] and this will be increasingly important if the patient is also taking CBD simultaneously not only due to a potential DDI but also due to the already compromised liver state and that chronic CBD administration leads to hepatoxicity [27]. The DDI simulations in cirrhotic patients in the present study saw a predicted morphine C_{max} of 49 ng/mL after coadministration of CBD. Hasselström et al. saw a morphine C_{max} of 29.4 ng/mL in cirrhotic patients and noted numerous side effects seen in the participants [44]. This suggests that a morphine concentration of 49 ng/mL would be even more likely to cause adverse side effects and necessitate dosage adjustments when taking both morphine and CBD. Furthermore, studies indicate that up to 30% of morphine glucuronidation occurs extrahepatically in cirrhotic patients compared to 10% in healthy volunteers [44,49]. This suggests that liver cirrhosis may not contribute to the potential DDI between morphine and CBD and that compensatory mechanisms are present to accommodate morphine metabolism when liver cirrhosis is present. This was observed in the DDI models in severe hepatic impairment in the present study—the renal contribution increased and subsequent renal CL_{int} decreased by 21.4% in the presence of CBD (Figure 5).

CBD exposure was also found to increase in mild, moderate, and severe HI patients [26]. The lack of increased morphine exposure in the HI virtual population in the presence of CBD is likely due to the CBD K_i value against UGT2B7. While the exposure of both morphine and CBD increased in cirrhotic populations, the overall inhibitory effect remained similar to that observed in healthy populations due to the K_i value being within physiological levels of CBD (though not for long periods of time based upon simulated CBD plasma concentration–time curves; Figure 3). It is likely that CBD is quickly metabolized by multiple enzymes (Supplemental Table S2), resulting in the concentrations of CBD being high enough to meet the K_i to exert an inhibitory effect on UGT2B7 only briefly.

Within the clinical studies used to develop and validate the morphine–CBD DDI models presented in this study, the mean morphine plasma concentration was 8.7 ng/mL and the mean simulated morphine concentration after coadministration with CBD was 14.8 ng/mL. The mean reported therapeutic window for morphine plasma concentrations is 9–80 ng/mL [53]. This suggests that toxicity and adverse side effects are seen when morphine

plasma concentrations exceed 80 ng/mL [54]. However, as described above, Hasselström et al. saw adverse side effects in morphine patients with a plasma concentration of 29 ng/mL [44]. This suggests that morphine-associated side effects can occur within the therapeutic window and vary between individuals due to several factors including opioid tolerance and natural steady-state concentrations. Thus, a mild increase in morphine exposure may still lead to adverse side effects due to interindividual variability in response to morphine. Furthermore, these studies do not report the brain tissue concentrations that correspond to the therapeutic window plasma concentrations of morphine.

Morphine has two primary metabolites, morphine-3-glucuronide and morphine-6-glucuronide. The models presented in this study did not predict the exposure of either metabolite in the presence of CBD. However, these models were able to describe a decrease in formation of both morphine-3-glucuronide and morphine-6-glucuronide due to the inhibition of UGT2B7. It has been reported that morphine-6-glucuronide contributes to the analgesic efficacy of morphine [8–10], and subsequent inhibition of metabolite formation would decrease its contribution to analgesia. However, the subsequent increase in morphine due to inhibition of UGT2B7-mediated metabolism to morphine-6-glucuronide may ameliorate the loss of contribution of analgesia from morphine-6-glucuronide. This requires future studies incorporating pharmacodynamic effects into the model. Furthermore, the decrease in morphine-3-glucuronide formation would be predicted to be beneficial as it is known to be neuroexcitatory and cause adverse side effects [7,8].

The disconnect between the current results and previous findings using static modeling may be because static modeling only considers a single concentration of the inhibitor (C_{max}) and thus is a worst-case scenario, whereas with PBPK modeling, the concentration of the inhibitor over time is considered and gives a more realistic prediction of the DDI potential between two or more compounds. PBPK modeling also allows prediction of tissue concentrations (i.e., liver or intestine) of the inhibitor to determine whether a perpetrator drug reaches high enough concentrations to cause a DDI, whereas static modeling is based on a single systemic concentration of an inhibitor (i.e., worst-case scenario).

The current study has several limitations. It is important to consider morphine and CBD use in a broader context where misuse may occur. For example, the DDI models reported in the present study may not accurately predict and assess DDI risk in individuals who are taking higher CBD doses. The current study performed predictive DDI models with a single week of multiple CBD doses that are higher than current dosing regimen strategies for Epidiolex™ [11], as pharmacokinetic studies for CBD at clinically relevant doses are not available. Therefore, the clinical data used for the present study may not represent the scenario of chronic CBD administration that individuals may use in terms of self-medicating doses of CBD or frequency of doses. Additional DDI simulations utilizing larger doses of CBD are needed to investigate the potential implications of high dose CBD-induced drug interactions with morphine. In addition, the models presented in this study did not incorporate the inhibitory effects of CBD's metabolites that have much larger exposures as compared to CBD itself. In previous studies, it was found that 7-OH-CBD also inhibited UGT2B7-mediated morphine metabolism [21]. Furthermore, 7-OH-CBD exposure is comparable to CBD exposure in healthy patients [54]. Thus, the potential for a DDI between CBD and morphine may be more severe than predicted by the data from the present study. A model incorporating CBD's metabolites would better characterize the inhibitory effect of concomitant usage of CBD and morphine. Also, the model did not incorporate the potential pharmacodynamic effects an increase in morphine exposure would have in either patient population. Future models can be developed to investigate the pharmacodynamic effects of inhibition of morphine UGT2B7-mediated metabolism by CBD and its major metabolites. Furthermore, only one study was available that measured CSF concentrations after morphine IV administration; therefore, the models presented in the present study could not be validated with another study for IV administration or in oral administration.

In summary, the present study is the first to investigate the potential DDI between morphine and CBD using PBPK modeling in two populations. CBD was shown to mildly increase morphine exposure (5–10%) in both healthy and cirrhotic populations after multiple doses of CBD. This increase in morphine exposure in our model was also seen in the brain tissue of virtual subjects in both populations. While results from this study show that concomitant use of CBD and morphine will likely not lead to a dramatic pharmacokinetic DDI, dosage adjustments and patient monitoring may be needed to ensure morphine plasma and brain concentrations remain within the narrow therapeutic window to ensure patient safety and efficacy. Future studies should also investigate the potential DDI between CBD and other commonly prescribed opioids either through PBPK modeling or clinical studies.

Supplementary Materials: The following supporting information can be downloaded at https://www.mdpi.com/article/10.3390/pharmaceutics16121599/s1, Figure S1: PBPK model of predicted and observed morphine plasma pharmacokinetic profiles after IV administration in healthy subjects. Data points represent the observed mean systemic plasma morphine concentrations (Stuart-Harris et al., 2000; Lotsch et al., 1998; Hoskin et al., 1989; Hasselstrom and Sawe, 1993; Osborne et al., 1990) [6,42,55–57] and the green line represents the model-predicted CBD plasma concentration–time profile. Gray lines indicate the 5th–95th percentile of the virtual population. Figure S2: PBPK model of predicted and observed plasma morphine pharmacokinetic profiles after (A) immediate release (Osborne et al., 1990; Masood et al., 1996; Hasselstrom and Sawe, 1993) [6,57,58] and (B) controlled release (Hoskin et al., 1989; Preechagoon et al., 2010; Kaiko et al., 1992; Drake et al., 1996) [37,42,59,60] oral administration healthy populations. Data points represent the observed mean systemic plasma morphine concentrations, and the green line represents the model-predicted CBD plasma concentration–time profile. Gray lines indicate the 5th–95th percentile of the virtual population. Figure S3: PBPK model of predicted and observed morphine CSF and brain concentrations after IV administration of 0.3 mg/kg of morphine in cancer patients (Meineke et al., 2002) [61]. Data points represent the observed values, and the green line represents the model-predicted morphine CSF or total brain concentration–time profiles. Gray lines indicate the 5th–95th percentile of the virtual population. Figure S4: PBPK model of predicted and observed CBD plasma pharmacokinetic profiles after IV administration of 20 mg CBD in healthy adults (Ohlsson et al., 1986) [62]. Data points represent the observed values, and the green line represents the model-predicted CBD plasma concentration–time profile. Gray lines indicate the 5th–95th percentile of the virtual population. Figure S5: PBPK model of predicted and observed (Taylor et al., 2018) [45] CBD plasma pharmacokinetic profiles after oral administration of CBD in healthy adults in the fasted state. Data points represent the observed mean systemic plasma CBD concentrations, and the green line represents the model-predicted CBD plasma concentration–time profile. Gray lines indicate the 5th–95th percentile of the virtual population. Figure S6: Sensitivity analysis for the change of inhibition constant (Ki) of CBD on the ratio of simulated morphine AUC. The horizontal black dashed line indicates the AUCR cutoff of 1.25 and the vertical red dashed line indicates the Ki value determined experimentally. Figure S7: Simulated morphine exposure with (red) and without (blue) CBD in (A) healthy, and (B) hepatic-impaired virtual populations, after oral administration of morphine (15.2 mg IR tablet) and CBD (1500 mg twice daily for 7 days). 95% confidence intervals are shaded. Table S1: Key physiochemical and system specific input parameters for the development of physiologically based pharmacokinetic model for morphine using Simcyp v23. Table S2: Key physiochemical and system specific input parameters for the development of physiologically based pharmacokinetic model for cannabidiol using Simcyp v23. Table S3: PBPK model-predicted and observed (mean and 90% CI) morphine exposure in healthy and cirrhotic adults after single intravenous or oral dose of morphine. Table S4: PBPK model-predicted and observed (mean and 90% CI) CBD exposure in healthy and cirrhotic adults after single intravenous or oral dose of CBD. References [6,22,23,26,29–33,35–38,40–45,55–66] are cited in the supplementary materials.

Author Contributions: Conceptualization, S.C. and P.L.; methodology, S.C., K.B., B.P. and P.L.; investigation, S.C.; formal analysis, S.C. and P.L.; visualization, S.C., K.B., B.P. and P.L.; validation, S.C.; writing—original draft, S.C. and P.L.; writing—review and editing, S.C., K.B., B.P. and P.L.; funding acquisition, S.C.; project administration, S.C. and P.L.; resources, S.C., B.P. and P.L.; supervision, S.C., B.P. and P.L. All authors have read and agreed to the published version of the manuscript.

Funding: This research was funded by a F31-DA056197 grant (to S. Coates) from the National Institute on Drug Abuse (NIDA). This paper is supported by the Alcohol and Drug Abuse Research Program (grant #2018F-ADARP) at Washington State University. This investigation was also supported in part by funds provided for medical and biological research by the State of Washington Initiative Measure No. 171.

Institutional Review Board Statement: Not applicable.

Informed Consent Statement: Not applicable.

Data Availability Statement: The original contributions presented in the study are included in the article/Supplementary Materials, further inquiries can be directed to the corresponding authors.

Conflicts of Interest: The authors declare no conflicts of interest.

References

1. Clark, J.D. Chronic pain prevalence and analgesic prescribing in a general medical population. *J. Pain Symptom Manag.* **2002**, *23*, 131–137. [CrossRef] [PubMed]
2. Manchikanti, L.; Abdi, S.; Atluri, S.; Balog, C.C.; Benyamin, R.M.; Boswell, M.V.; Brown, K.R.; Bruel, B.M.; Bryce, D.A.; Burks, P.A.; et al. American Society of Interventional Pain Physicians (ASIPP) guidelines for responsible opioid prescribing in chronic non-cancer pain: Part I—Evidence assessment. *Pain Physician* **2012**, *15*, S1–S65. [PubMed]
3. Wiffen, P.J.; Wee, B.; Derry, S.; Bell, R.F.; Moore, R.A. Opioids for cancer pain-an overview of Cochrane reviews. *Cochrane Database Syst. Rev.* **2017**, *2017*, CD012592. [CrossRef]
4. Stone, A.N.; Mackenzie, P.I.; Galetin, A.; Houston, J.B.; Miners, J.O. Isoform selectivity and kinetics of morphine 3- and 6-glucuronidation by human udp-glucuronosyltransferases: Evidence for atypical glucuronidation kinetics by UGT2B7. *Drug Metab. Dispos.* **2003**, *31*, 1086–1089. [CrossRef]
5. Coffman, B.L.; Rios, G.R.; King, C.D.; Tephly, T.R. Human UGT2B7 catalyzes morphine glucuronidation. *Drug Metab. Dispos.* **1997**, *25*, 1–4.
6. Hasselström, J.; Säwe, J. Morphine pharmacokinetics and metabolism in humans. Enterohepatic cycling and relative contribution of metabolites to active opioid concentrations. *Clin. Pharmacokinet.* **1993**, *24*, 344–354. [CrossRef] [PubMed]
7. Roeckel, L.A.; Utard, V.; Reiss, D.; Mouheiche, J.; Maurin, H.; Robé, A.; Audouard, E.; Wood, J.N.; Goumon, Y.; Simonin, F.; et al. Morphine-induced hyperalgesia involves mu opioid receptors and the metabolite morphine-3-glucuronide. *Sci. Rep.* **2017**, *7*, 10406. [CrossRef]
8. Wittwer, E.; Kern, S.E. Role of morphine's metabolites in analgesia: Concepts and controversies. *AAPS J.* **2006**, *8*, E348–E352. [CrossRef]
9. Kilpatrick, G.J.; Smith, T.W. Morphine-6-glucuronide: Actions and mechanisms. *Med. Res. Rev.* **2005**, *25*, 521–544. [CrossRef] [PubMed]
10. Frances, B.; Gout, R.; Monsarrat, B.; Cros, J.; Zajac, J.M. Further evidence that morphine-6 beta-glucuronide is a more potent opioid agonist than morphine. *J. Pharmacol. Exp. Ther.* **1992**, *262*, 25–31. [PubMed]
11. Greenwich Biosciences, Inc. *Epidiolex*; Greenwich Biosciences, Inc.: Carlsbad, CA, USA, 2020. Available online: https://www.accessdata.fda.gov/drugsatfda_docs/label/2020/210365s005s006s007lbl.pdf (accessed on 18 December 2023).
12. Corroon, J.; Phillips, J.A. A Cross-Sectional Study of Cannabidiol Users. *Cannabis Cannabinoid Res.* **2018**, *3*, 152–161. [CrossRef]
13. Moltke, J.; Hindocha, C. Reasons for cannabidiol use: A cross-sectional study of CBD users, focusing on self-perceived stress, anxiety, and sleep problems. *J. Cannabis Res.* **2021**, *3*, 5. [CrossRef]
14. Sexton, M.; Cuttler, C.; Finnell, J.S.; Mischley, L.K. A Cross-Sectional Survey of Medical Cannabis Users: Patterns of Use and Perceived Efficacy. *Cannabis Cannabinoid Res.* **2016**, *1*, 131–138. [CrossRef]
15. Wilson, M.; Gogulski, H.Y.; Cuttler, C.; Bigand, T.L.; Oluwoye, O.; Barbosa-Leiker, C.; Roberts, M.A. Cannabis use moderates the relationship between pain and negative affect in adults with opioid use disorder. *Addict. Behav.* **2018**, *77*, 225–231. [CrossRef]
16. Clem, S.N.; Bigand, T.L.; Wilson, M. Cannabis Use Motivations among Adults Prescribed Opioids for Pain versus Opioid Addiction. *Pain Manag. Nurs.* **2020**, *21*, 43–47. [CrossRef]
17. Mahabir, V.K.; Merchant, J.J.; Smith, C.; Garibaldi, A. Medical cannabis use in the United States: A retrospective database study. *J. Cannabis Res.* **2020**, *2*, 32. [CrossRef] [PubMed]
18. Nasrin, S.; Watson, C.J.W.; Perez-Paramo, Y.X.; Lazarus, P. Cannabinoid Metabolites as Inhibitors of Major Hepatic CYP450 Enzymes, with Implications for Cannabis-Drug Interactions. *Drug Metab. Dispos.* **2021**, *49*, 1070–1080. [CrossRef] [PubMed]
19. Nasrin, S.; Watson, C.J.W.; Bardhi, K.; Fort, G.; Chen, G.; Lazarus, P. Inhibition of UDP-Glucuronosyltransferase Enzymes by Major Cannabinoids and Their Metabolites. *Drug Metab. Dispos.* **2021**, *49*, 1081–1089. [CrossRef] [PubMed]
20. Bardhi, K.; Coates, S.; Chen, G.; Lazarus, P. Cannabinoid-Induced Stereoselective Inhibition of R-S-Oxazepam Glucuronidation: Cannabinoid–Oxazepam Drug Interactions. *Pharmaceutics* **2024**, *16*, 243. [CrossRef] [PubMed]
21. Coates, S.; Bardhi, K.; Lazarus, P. Cannabinoid-Induced Inhibition of Morphine Glucuronidation and the Potential for In Vivo Drug–Drug Interactions. *Pharmaceutics* **2024**, *16*, 418. [CrossRef] [PubMed]

22. Bansal, S.; Maharao, N.; Paine, M.F.; Unadkat, J.D. Predicting the Potential for Cannabinoids to Precipitate Pharmacokinetic Drug Interactions via Reversible Inhibition or Inactivation of Major Cytochromes P450. *Drug Metab. Dispos.* **2020**, *48*, 1008–1017. [CrossRef] [PubMed]
23. Bansal, S.; Paine, M.F.; Unadkat, J.D. Comprehensive Predictions of Cytochrome P450 (P450)-Mediated In Vivo Cannabinoid-Drug Interactions Based on Reversible and Time-Dependent P450 Inhibition in Human Liver Microsomes. *Drug Metab. Dispos.* **2022**, *50*, 351–360. [CrossRef]
24. Grimstein, M.; Yang, Y.; Zhang, X.; Grillo, J.; Huang, S.M.; Zineh, I.; Wang, Y. Physiologically Based Pharmacokinetic Modeling in Regulatory Science: An Update From the U.S. Food and Drug Administration's Office of Clinical Pharmacology. *J. Pharm. Sci.* **2019**, *108*, 21–25. [CrossRef] [PubMed]
25. US Food and Drug Administration. *Physiologically Based Pharmacokinetic Analyses–Format and Content Guidance for Industry*; Center for Drug Evaluation and Research: Silver Spring, MD, USA, 2018; pp. 1–9.
26. Taylor, L.; Crockett, J.; Tayo, B.; Morrison, G. A Phase 1, Open-Label, Parallel-Group, Single-Dose Trial of the Pharmacokinetics and Safety of Cannabidiol (CBD) in Subjects With Mild to Severe Hepatic Impairment. *J. Clin. Pharmacol.* **2019**, *59*, 1110–1119. [CrossRef] [PubMed]
27. Watkins, P.B.; Church, R.J.; Li, J.; Knappertz, V. Cannabidiol and Abnormal Liver Chemistries in Healthy Adults: Results of a Phase I Clinical Trial. *Clin. Pharmacol. Ther.* **2021**, *109*, 1224–1231. [CrossRef]
28. U.S. Food and Drug Administration. Epidiolex NDA 210365Origs000 Labeling; 25 June 2018; pp. 1–32. Available online: https://www.accessdata.fda.gov/drugsatfda_docs/nda/2018/210365Orig1s000OtherR.pdf (accessed on 30 August 2023).
29. Emoto, C.; Fukuda, T.; Johnson, T.; Neuhoff, S.; Sadhasivam, S.; Vinks, A. Characterization of Contributing Factors to Variability in Morphine Clearance Through PBPK Modeling Implemented With OCT1 Transporter. *CPT Pharmacomet. Syst. Pharmacol.* **2017**, *6*, 110–119. [CrossRef] [PubMed]
30. Uchaipichat, V.; Rowland, A.; Miners, J.O. Inhibitory effects of non-steroidal anti-inflammatory drugs on human liver microsomal morphine glucuronidation: Implications for drug-drug interaction liability. *Drug Metab. Pharmacokinet.* **2022**, *42*, 100442. [CrossRef] [PubMed]
31. Rodgers, T.; Leahy, D.; Rowland, M. Physiologically based pharmacokinetic modeling 1: Predicting the tissue distribution of moderate-to-strong bases. *J. Pharm. Sci.* **2005**, *94*, 1259–1276. [CrossRef]
32. Rodgers, T.; Rowland, M. Physiologically based pharmacokinetic modelling 2: Predicting the tissue distribution of acids, very weak bases, neutrals and zwitterions. *J. Pharm. Sci.* **2006**, *95*, 1238–1257. [CrossRef] [PubMed]
33. Jamei, M.; Bajot, F.; Neuhoff, S.; Barter, Z.; Yang, J.; Rostami-Hodjegan, A.; Rowland-Yeo, K. A Mechanistic Framework for In Vitro–In Vivo Extrapolation of Liver Membrane Transporters: Prediction of Drug–Drug Interaction Between Rosuvastatin and Cyclosporine. *Clin. Pharmacokinet.* **2014**, *53*, 73–87. [CrossRef]
34. Neuhoff, S.; Yeo, K.R.; Barter, Z.; Jamei, M.; Turner, D.B.; Rostami-Hodjegan, A. Application of permeability-limited physiologically-based pharmacokinetic models: Part II-prediction of p-glycoprotein mediated drug–drug interactions with digoxin. *J. Pharm. Sci.* **2013**, *102*, 3161–3173. [CrossRef] [PubMed]
35. Tzvetkov, M.V.; dos Santos Pereira, J.N.; Meineke, I.; Saadatmand, A.R.; Stingl, J.C.; Brockmöller, J. Morphine is a substrate of the organic cation transporter OCT1 and polymorphisms in OCT1 gene affect morphine pharmacokinetics after codeine administration. *Biochem. Pharmacol.* **2013**, *86*, 666–678. [CrossRef]
36. Krekels, E.H.; Johnson, T.N.; den Hoedt, S.M.; Rostami-Hodjegan, A.; Danhof, M.; Tibboel, D.; Knibbe, C.A. From Pediatric Covariate Model to Semiphysiological Function for Maturation: Part II-Sensitivity to Physiological and Physicochemical Properties. *CPT Pharmacomet. Syst. Pharmacol.* **2012**, *1*, e10. [CrossRef]
37. Preechagoon, D.; Sumyai, V.; Chulavatnatol, S.; Kulvanich, P.; Tessiri, T.; Tontisirin, K.; Pongjanyakul, T.; Uchaipichat, V.; Aumpon, S.; Wongvipaporn, C. Formulation Development of Morphine Sulfate Sustained-Release Tablets and Its Bioequivalence Study in Healthy Thai Volunteers. *AAPS PharmSciTech* **2010**, *11*, 1449–1455. [CrossRef] [PubMed]
38. Verscheijden, L.F.M.; Litjens, C.H.C.; Koenderink, J.B.; Mathijssen, R.H.J.; Verbeek, M.M.; de Wildt, S.N.; Russel, F.G.M. Physiologically based pharmacokinetic/pharmacodynamic model for the prediction of morphine brain disposition and analgesia in adults and children. *PLoS Comput. Biol.* **2021**, *17*, e1008786. [CrossRef]
39. Gaohua, L.; Neuhoff, S.; Johnson, T.N.; Rostami-Hodjegan, A.; Jamei, M. Development of a permeability-limited model of the human brain and cerebrospinal fluid (CSF) to integrate known physiological and biological knowledge: Estimating time varying CSF drug concentrations and their variability using in vitro data. *Drug Metab. Pharmacokinet.* **2016**, *31*, 224–233. [CrossRef]
40. Bansal, S.; Ladumor, M.K.; Paine, M.F.; Unadkat, J.D. A Physiologically-Based Pharmacokinetic Model for Cannabidiol in Healthy Adults, Hepatically-Impaired Adults, and Children. *Drug Metab. Dispos.* **2023**, *51*, 743–752. [CrossRef] [PubMed]
41. Lötsch, J.; Skarke, C.; Schmidt, H.; Liefhold, J.; Geisslinger, G. Pharmacokinetic modeling to predict morphine and morphine-6-glucuronide plasma concentrations in healthy young volunteers. *Clin. Pharmacol. Ther.* **2002**, *72*, 151–162. [CrossRef]
42. Hoskin, P.J.; Hanks, G.W.; Aherne, G.W.; Chapman, D.; Littleton, P.; Filshie, J. The bioavailability and pharmacokinetics of morphine after intravenous, oral and buccal administration in healthy volunteers. *Br. J. Clin. Pharmacol.* **1989**, *27*, 499–505. [CrossRef] [PubMed]
43. Kotb, H.I.; El-Kady, S.A.; Emara, S.E.; Fouad, E.A.; El-Kabsh, M.Y. Pharmacokinetics of controlled release morphine (MST) in patients with liver carcinoma. *Br. J. Anaesth.* **2005**, *94*, 95–99. [CrossRef] [PubMed]

44. Hasselström, J.; Eriksson, S.; Persson, A.; Rane, A.; Svensson, J.O.; Säwe, J. The metabolism and bioavailability of morphine in patients with severe liver cirrhosis. *Br. J. Clin. Pharmacol.* **1990**, *29*, 289–297. [CrossRef]
45. Taylor, L.; Gidal, B.; Blakey, G.; Tayo, B.; Morrison, G. A Phase I, Randomized, Double-Blind, Placebo-Controlled, Single Ascending Dose, Multiple Dose, and Food Effect Trial of the Safety, Tolerability and Pharmacokinetics of Highly Purified Cannabidiol in Healthy Subjects. *CNS Drugs* **2018**, *32*, 1053–1067. [CrossRef] [PubMed]
46. FDA. *In Vitro Drug Interaction Studies-Cytochrome P450 Enzyme-and Transporter-Mediated Drug Interactions Guidance for Industry*; FDA: Silver Spring, MD, USA, 2020; pp. 1–46.
47. Milne, R.W.; Nation, R.L.; Somogyi, A.A. The disposition of morphine and its 3- and 6-glucuronide metabolites in humans and animals, and the importance of the metabolites to the pharmacological effects of morphine. *Drug Metab. Rev.* **1996**, *28*, 345–472. [CrossRef]
48. El-Khateeb, E.; Achour, B.; Al-Majdoub, Z.M.; Barber, J.; Rostami-Hodjegan, A. Non-uniformity of Changes in Drug-Metabolizing Enzymes and Transporters in Liver Cirrhosis: Implications for Drug Dosage Adjustment. *Mol. Pharm.* **2021**, *18*, 3563–3577. [CrossRef] [PubMed]
49. Crotty, B.; Watson, K.J.; Desmond, P.V.; Mashford, M.L.; Wood, L.J.; Colman, J.; Dudley, F.J. Hepatic extraction of morphine is impaired in cirrhosis. *Eur. J. Clin. Pharmacol.* **1989**, *36*, 501–506. [CrossRef] [PubMed]
50. Kotb, H.I.; el-Kabsh, M.Y.; Emara, S.E.; Fouad, E.A. Pharmacokinetics of controlled release morphine (MST) in patients with liver cirrhosis. *Br. J. Anaesth.* **1997**, *79*, 804–806. [CrossRef]
51. Mazoit, J.X.; Sandouk, P.; Zetlaoui, P.; Scherrmann, J.M. Pharmacokinetics of unchanged morphine in normal and cirrhotic subjects. *Anesth. Analg.* **1987**, *66*, 293–298. [CrossRef]
52. Pathwardhan, R.V.; Johnsson, R.F.; Hoyumpa, A.J.; Sheehan, J.J.; Desmond, P.V.; Wilkinson, G.R.; Branch, R.A.; Schenker, S. Normal metabolism of morphine in cirrhosis. *Gastroenterology* **1981**, *81*, 1006–1011. [CrossRef]
53. Gourlay, G.K.; Willis, R.J.; Lamberty, J. A Double-blind Comparison of the Efficacy of Methadone and Morphine in Postoperative Pain Control. *Anesthesiology* **1986**, *64*, 322–327. [CrossRef]
54. Linares, O.A.; Linares, A.L. Computational Opioid Prescribing: A Novel Application of Clinical Pharmacokinetics. *J. Pain. Palliat. Care Pharmacother.* **2011**, *25*, 125–135. [CrossRef] [PubMed]
55. Stuart-Harris, R.; Joel, S.P.; McDonald, P.; Currow, D.; Slevin, M.L. The pharmacokinetics of morphine and morphine glucuronide metabolites after subcutaneous bolus injection and subcutaneous infusion of morphine. *Br. J. Clin. Pharmacol.* **2000**, *49*, 207–214. [CrossRef] [PubMed]
56. Lötsch, J.; Weiss, M.; Kobal, G.; Geisslinger, G. Pharmacokinetics of morphine-6-glucuronide and its formation from morphine after intravenous administration. *Clin. Pharmacol. Ther.* **1998**, *63*, 629–639. [CrossRef] [PubMed]
57. Osborne, R.; Joel, S.; Trew, D.; Slevin, M. Morphine and metabolite behavior after different routes of morphine administration: Demonstration of the importance of the active metabolite morphine-6-glucuronide. *Clin. Pharmacol. Ther.* **1990**, *47*, 12–19. [CrossRef]
58. Masood, A.R.; Thomas, S.H. Systemic absorption of nebulized morphine compared with oral morphine in healthy subjects. *Br. J. Clin. Pharmacol.* **1996**, *41*, 250–252. [CrossRef]
59. Kaiko, R.F.; Fitzmartin, R.D.; Thomas, G.B.; Goldenheim, P.D. The bioavailability of morphine in controlled-release 30-mg tablets per rectum compared with immediate-release 30-mg rectal suppositories and controlled-release 30-mg oral tablets. *Pharmacotherapy* **1992**, *12*, 107–113. [CrossRef]
60. Drake, J.; Kirkpatrick, C.T.; Aliyar, C.A.; Crawford, F.E.; Gibson, P.; Horth, C.E. Effect of food on the comparative pharmacokinetics of modified-release morphine tablet formulations: Oramorph SR and MST Continus. *Br. J. Clin. Pharmacol.* **1996**, *41*, 417–420. [CrossRef]
61. Meineke, I.; Freudenthaler, S.; Hofmann, U.; Schaeffeler, E.; Mikus, G.; Schwab, M.; Prange, H.W.; Gleiter, C.H.; Brockmöller, J. Pharmacokinetic modelling of morphine, morphine-3-glucuronide and morphine-6-glucuronide in plasma and cerebrospinal fluid of neurosurgical patients after short-term infusion of morphine. *Br. J. Clin. Pharmacol.* **2002**, *54*, 592–603. [CrossRef]
62. Ohlsson, A.; Lindgren, J.E.; Andersson, S.; Agurell, S.; Gillespie, H.; Hollister, L.E. Single-dose kinetics of deuterium-labelled cannabidiol in man after smoking and intravenous administration. *Biomed. Environ. Mass Spectrom.* **1986**, *13*, 77–83. [CrossRef]
63. Poulin, P.; Theil, F.P. Prediction of pharmacokinetics prior to in vivo studies. 1. Mechanism-based prediction of volume of distribution. *J. Pharm. Sci.* **2002**, *91*, 129–156. [CrossRef]
64. Samara, E.; Bialer, M.; Mechoulam, R. Pharmacokinetics of cannabidiol in dogs. *Drug Metab. Dispos.* **1988**, *16*, 469–472. [PubMed]
65. Tayo, B.; Taylor, L.; Sahebkar, F.; Morrison, G. A Phase I, Open-Label, Parallel-Group, Single-Dose Trial of the Pharmacokinetics, Safety, and Tolerability of Cannabidiol in Subjects with Mild to Severe Renal Impairment. *Clin. Pharmacokinet.* **2020**, *59*, 747–755. [CrossRef] [PubMed]
66. Zdrazil, B.; Felix, E.; Hunter, F.; Manners, E.J.; Blackshaw, J.; Corbett, S.; de Veij, M.; Ioannidis, H.; Lopez, D.M.; Mosquera, J.F.; et al. The ChEMBL Database in 2023: A drug discovery platform spanning multiple bioactivity data types and time periods. *Nucleic Acids Res.* **2024**, *52*, D1180–D1192. [CrossRef] [PubMed]